

# Nanosieving of Anions and Cavity-Size-Dependent Association of Cyclodextrins on a 1-Adamantanethiol Self-Assembled Monolayer

Jun Hui Park,<sup>†,§</sup> Seongpil Hwang,<sup>‡,§,\*</sup> and Juhyoun Kwak<sup>†,\*</sup>

<sup>†</sup>Molecular-Level Interface Research Center, Department of Chemistry, KAIST, Daejeon 305-701, Republic of Korea, and <sup>‡</sup>Department of Chemistry, Myongji University, Yongin 449-728, Republic of Korea. <sup>§</sup>These authors contributed equally to this work.

Adamantane, which comprises a 10-carbon cage formed by four fused cyclohexane rings in chair conformation, is the simplest diamondoid.<sup>1</sup> 1-Adamantanethiol, shown in Scheme 1a, is an adamantane derivative with a thiol functional group at the 1 carbon position. It can form a self-assembled monolayer (SAM) on gold surfaces *via* a sulfur–gold bond, which has been used to construct well-ordered films over the past two decades.<sup>2</sup> Upon immersion, alkanethiol molecules spontaneously produce compact and well-ordered monolayers on gold due to the strong bonds between gold and the thiol group and by van der Waals interactions between the alkane chains. Similarly, 1-adamantanethiol adsorbs onto gold surfaces to generate highly packed hexagonal monolayers on Au(111) with defect densities that are lower than those of alkanethiol SAMs.<sup>3,4</sup> In contrast with the linear alkanethiol SAMs, adsorbed 1-adamantanethiol is readily displaced by other alkanethiols.<sup>4–7</sup> The lability may result from a reduction in the van der Waals interactions because neighboring adamantane molecules are separated by a relatively large distance due to their bulky size. 1-Adamantanethiol has a footprint on gold of 38.9 Å<sup>2</sup>/molecule, much larger than that of the short alkanethiol, 21.4 Å<sup>2</sup>/molecule, demonstrating that the short linear alkanethiols can be packed 1.8 times more densely than 1-adamantanethiol.<sup>6</sup> The thermodynamics of the molecular exchange were explained by a combination of energetically favorable contributions from an increase in the number of gold–sulfur bonds and an increase in the strength of the van

**ABSTRACT** In this paper, we studied charge transfer through a self-assembled monolayer (SAM) of 1-adamantanethiol on gold. Charge transfer through the 1-adamantanethiol SAM depended on the type of anion present when [Fe(CN)<sub>6</sub>]<sup>3–</sup> was used as a redox probe. The sluggish charge transfer process was monitored by cyclic voltammetry using the relatively large and hydrophobic perchlorate and hexafluorophosphate ions as the supporting electrolyte. In contrast, the charge transfer kinetics were nearly identical to those measured on bare gold with chloride, sulfate, and nitrate ions as the supporting electrolyte. We investigated the adsorption of  $\alpha$ - and  $\beta$ -cyclodextrin on the 1-adamantanethiol SAM *via* a host–guest interaction. The 1-adamantanethiol SAM could not bind  $\beta$ -cyclodextrin *via* a host–guest interaction, probably due to the proximity of neighboring adamantane molecules on the surface. Immobilization of  $\alpha$ -cyclodextrin by formation of an exterior complex with the SAM suppressed charge transfer. The adsorbed  $\alpha$ -cyclodextrin was quantified using faradaic impedance experiments. The obtained adsorption isotherm was in good agreement with the Langmuir isotherm with a binding constant of 39.53 M<sup>–1</sup>.

**KEYWORDS:** adamantane · adamantanethiol · cyclodextrin · host–guest interaction · sieving behavior

der Waals interactions.<sup>6</sup> Tethered 1-adamantanethiol on gold can thus be easily exchanged with other alkanethiols. Recently, the Weiss group reported enhanced microcontact printing (microdisplacement printing) in which alkanethiol ink was printed onto a preformed 1-adamantanethiol SAM to minimize the lateral diffusion of alkanethiols during printing.<sup>8</sup> Microdisplacement printing enables the printing of a variety of molecules *via* microcontact printing<sup>9,10</sup> and provides increased resolution and stability.

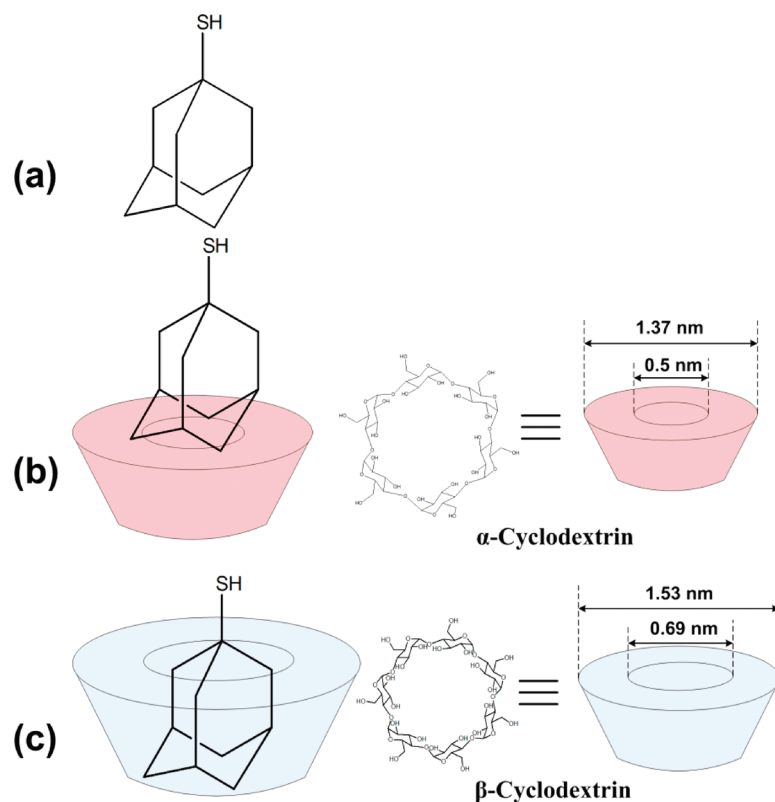
The host–guest chemistry of adamantane and cyclodextrin derivatives, which is important in drug delivery systems, separation systems, and in the food industry,<sup>11</sup> is an important property of adamantane.  $\alpha$ -Cyclodextrin is composed of six  $\alpha$ -D-glucose units linked together by  $\alpha$ -1,4-glycosidic bonds, and  $\beta$ -cyclodextrin is

\*Address correspondence to juhyoun\_kwak@kaist.ac.kr, shwang@mju.ac.kr.

Received for review April 22, 2010 and accepted June 22, 2010.

Published online June 29, 2010. 10.1021/nn1008484

© 2010 American Chemical Society



**Scheme 1.** (a) Structure of 1-adamantanethiol. Schemes of (b) the exterior complex of 1-adamantanethiol with  $\alpha$ -cyclodextrin, and (c) inclusion of  $\beta$ -cyclodextrin.

composed of seven residues. These oligosaccharides form a truncated cone that resembles a torus with varying diameter, depending on the number of units. The interior of the torus is hydrophobic, and the outer torus is hydrophilic, making the molecule highly water-soluble. As a result, cyclodextrins form inclusion complexes and act as hosts to hydrophobic guest molecules that are accommodated within the toroid, as shown in Scheme 1b,c. Nonpolar adamantane intrudes into the hydrophobic central cavity of  $\alpha$ -cyclodextrin and  $\beta$ -cyclodextrin with association constants on the order of  $10^2$  and  $10^4 \text{ M}^{-1}$ , respectively.<sup>12</sup> The association constant with  $\beta$ -cyclodextrin is larger primarily due to the complementarity of the fit of the adamantane ring, with a diameter of 0.69 nm, into the cavity of  $\beta$ -cyclodextrin, which has an estimated average diameter of 0.69 nm.<sup>12</sup>  $\alpha$ -Cyclodextrin has a smaller cavity with an estimated diameter of 0.5 nm so that adamantane cannot be accommodated as deeply as in  $\beta$ -cyclodextrin. Computational and NMR studies of the structure of  $\alpha$ -cyclodextrin and an adamantane derivative have shown that the guest is positioned outside the torus and forms an exterior complex with a smaller association constant.<sup>13</sup> The host–guest interaction of adamantane derivatives with cyclodextrins on a surface has also been studied. The association constants of guest molecules with surface-tethered  $\alpha$ -cyclodextrin molecules were 2–5 times smaller than the association constants of the molecules free in solution.<sup>14</sup> Galla and

co-workers reported an interfacial association constant with 1-adamantanammonium and 1-adamantanecarboxylate ions at a gold electrode modified with a monolayer of mono-6-(3-mercaptopropionamide)-6-deoxy- $\beta$ -cyclodextrin.<sup>15</sup> The host–guest chemistry of cyclodextrins has been exploited in a variety of applications in recent years. Several researchers have applied this complexation reaction in electrochemical sensors<sup>16</sup> and in the construction of enzyme multilayers,<sup>17</sup> nanoparticles,<sup>18</sup> and dendrimers.<sup>19</sup> This type of noncovalent supramolecular interaction facilitates the controlled assembly of building blocks on a surface.

The electrochemical properties and the binding with cyclodextrins of the 1-adamantanethiol SAM on gold, however, have not been reported, despite recent reports of its use in microdisplacement printing and host–guest interactions. Here we report the anion-dependent charge transfer caused by nanosieving and the association of cyclodextrins on 1-adamantanethiol SAMs. The degree of sluggish charge transfer to the redox probe molecules in solution was monitored by cyclic voltammetry in the presence of a variety of supporting electrolyte anions. The effect of surface tethering of the guest molecules on binding to cyclodextrins was examined, and the association constant of  $\alpha$ -cyclodextrin with the 1-adamantanethiol SAM was determined by cyclic voltammetry and faradaic impedance experiments. These experiments demonstrated

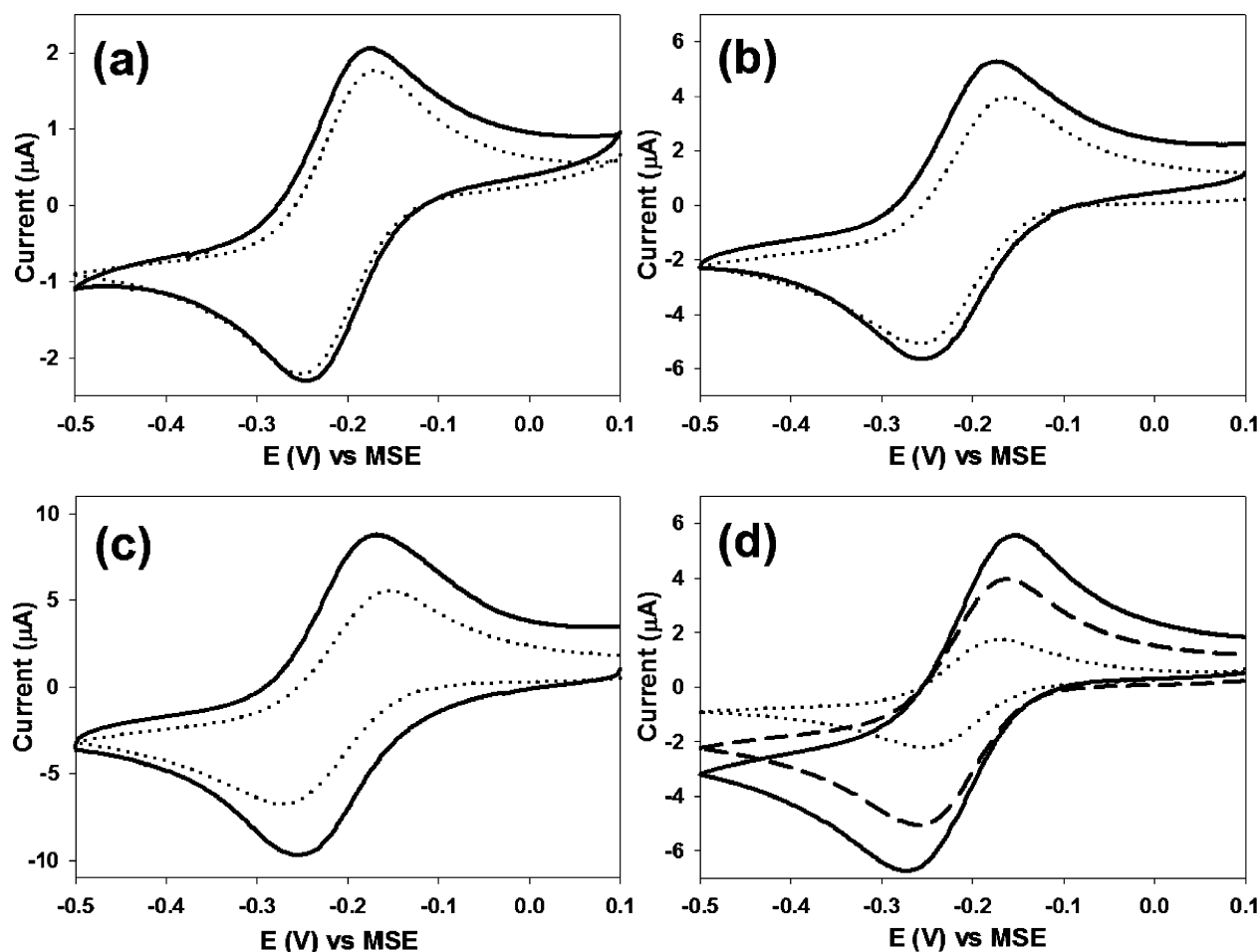


Figure 1. (a–c) Cyclic voltammograms (CVs) for the redox reaction of 0.1 mM  $\text{Fe}(\text{CN})_6^{3-}$  containing 0.1 M  $\text{KClO}_4$  on a bare gold electrode (solid line) and on a 1-adamantanethiol SAM-modified gold surface (dotted line) with scan rates of (a) 10 mV/s, (b) 50 mV/s, and (c) 100 mV/s. (d) CVs for the redox reaction of 0.1 mM  $\text{Fe}(\text{CN})_6^{3-}$  on 1-adamantanethiol SAM-modified gold at various scan rates: 10 mV/s (dotted line), 50 mV/s (dashed line), and (c) 100 mV/s (solid line).

the unique electrochemical properties of the 1-adamantanethiol SAM.

## RESULTS AND DISCUSSION

**Electrochemical Properties of the 1-Adamantanethiol SAM on Gold.** To investigate charge transfer through a SAM composed of 1-adamantanethiol, we chose  $\text{K}_3[\text{Fe}(\text{CN})_6]$  as the redox probe and performed cyclic voltammetry on the systems. Figure 1 shows the cyclic voltammograms (CVs) for the redox reaction of ferricyanide on the 1-adamantanethiol SAM-modified gold at various scan rates in the solution containing  $\text{KClO}_4$ . At a slow scan rate of 10 mV/s, the CV was almost identical to that observed on bare gold, although the currents at the redox peaks were slightly lower, as shown in Figure 1a. The presence of 1-adamantanethiol, however, reduced the faradaic currents and slowed the kinetics, as indicated by the increasing peak separation and decreasing peak currents at higher scan rates, shown in Figure 1b,c. These results demonstrated that the blocking behavior of 1-adamantanethiol appears more clearly at faster scan rates. The CVs indicated that charge transfer of ferricyanide on the 1-adamantanethiol SAM-

modified gold surface was electrochemically quasi-reversible because the shape of the peaks in Figure 1d changed as a function of the scan rate.<sup>20</sup> Previously, the Weiss group reported that the CV for the redox reaction of ferricyanide on the 1-adamantanethiol SAM was almost indistinguishable from that on a bare gold surface, even with a fast scan rate of 100 mV/s. They concluded that the 1-adamantanethiol SAM did not block the redox reaction of ferricyanide despite the presence of a well-ordered monolayer.<sup>21</sup> They suggested that charge transfer through the SAM was not blocked due to the increased lateral distance between adamantanes, decreased intermolecular interactions, and smaller physical size of 1-adamantanethiols. The only difference between our experiment and those previously reported is the composition of the supporting electrolyte. The dependence of charge transfer to ferricyanide, through the 1-adamantanethiol SAM, on the composition of the electrolyte was predicted on the basis of the electrochemical measurements.

Figure 2 shows the CVs for the redox reaction of ferricyanide on the 1-adamantanethiol-modified gold surface using several salts as the supporting electrolyte.

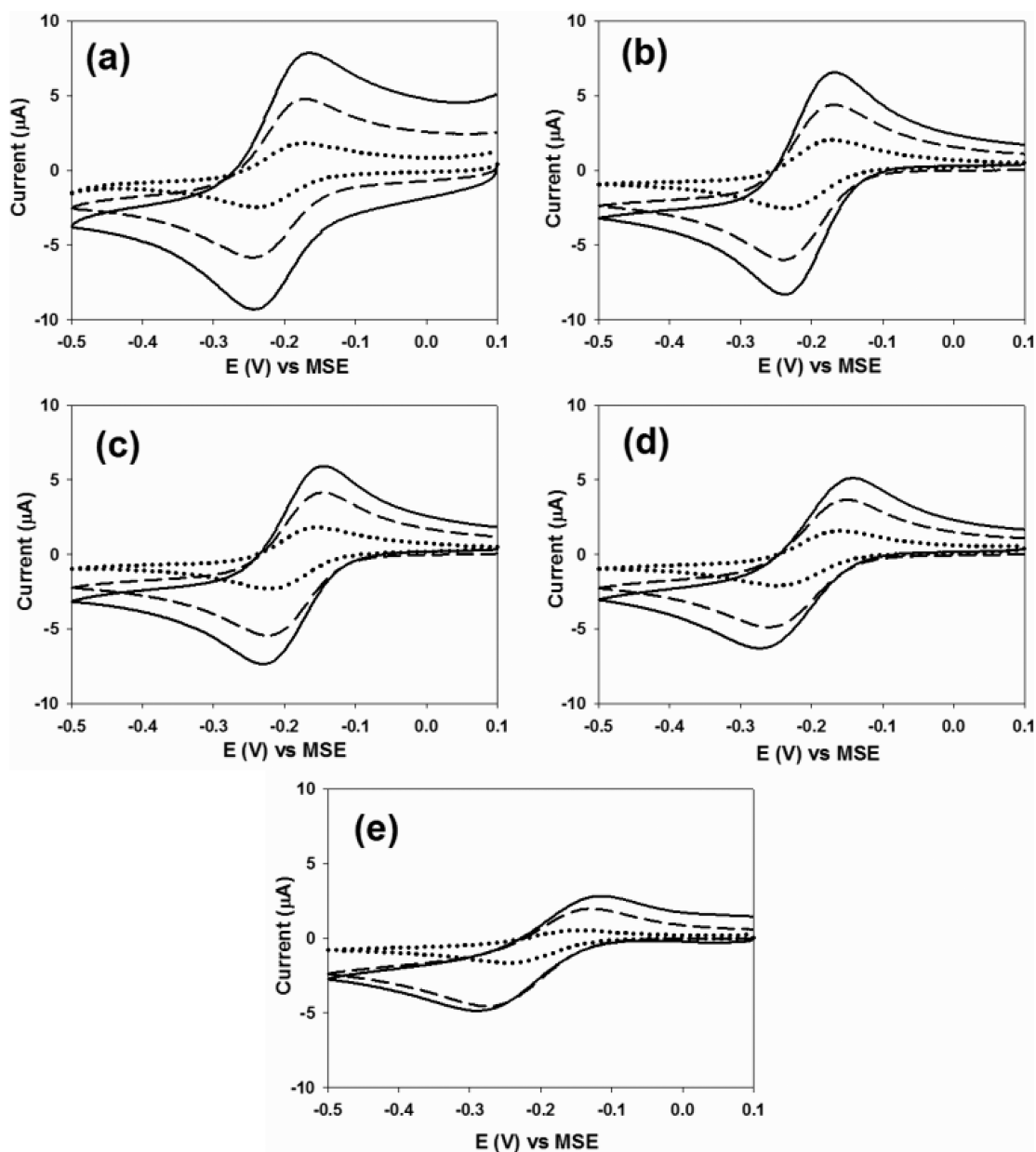
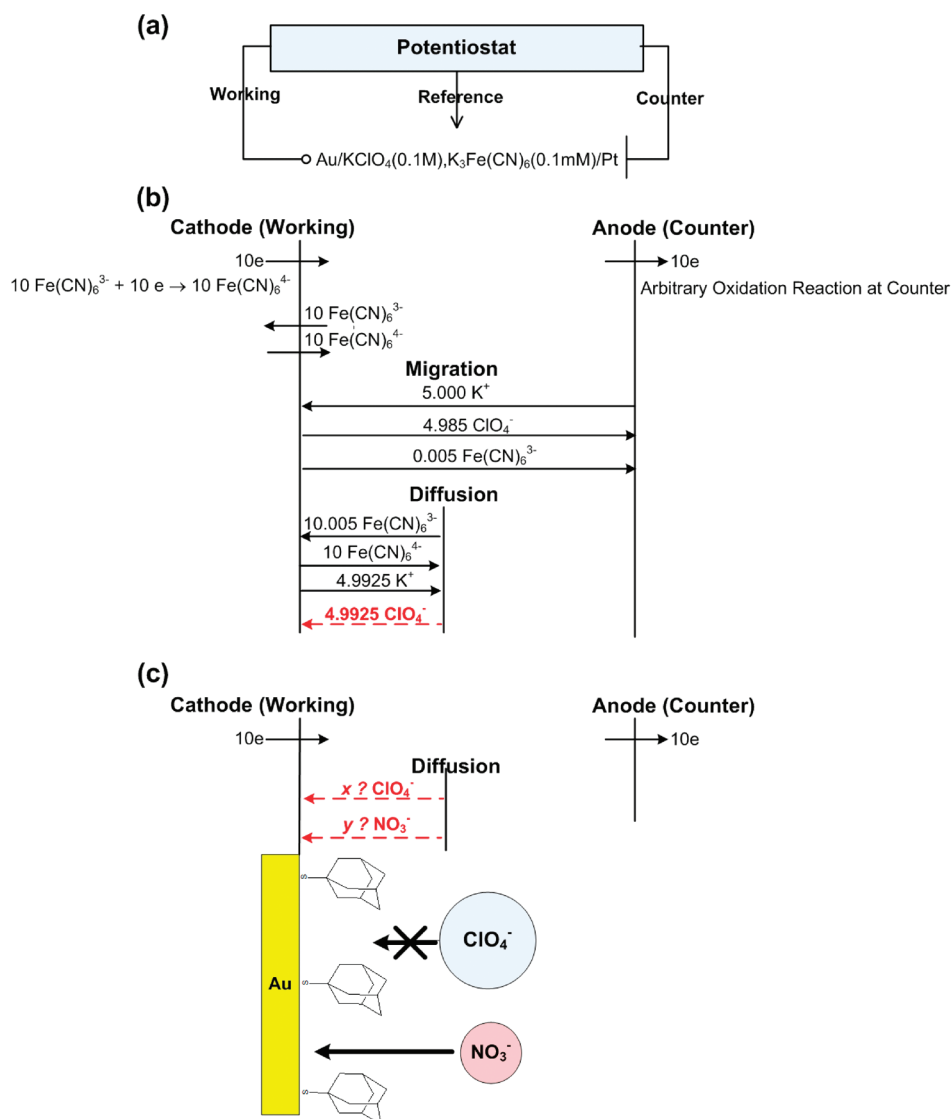


Figure 2. CVs for the redox reaction of 0.1 mM  $\text{Fe}(\text{CN})_6^{3-}$  with different supporting electrolytes: (a) 0.1 M KCl, (b) 0.1 M  $\text{K}_2\text{SO}_4$ , (c) 0.1 M  $\text{KNO}_3$ , (d) 0.1 M  $\text{KClO}_4$ , and (e) 0.1 M  $\text{KPF}_6$  on 1-adamantanethiol SAM-modified gold at various scan rates: 10 mV/s (dotted line), 50 mV/s (dashed line), and (c) 100 mV/s (solid line).

The voltammetric response was very similar in the solution containing KCl, as shown in Figure 2a, in good agreement with a previous report.<sup>21</sup> Peak separation and peak currents demonstrated electrochemically reversible charge transfer in a solution containing  $\text{K}_2\text{SO}_4$  (Figure 2b) and  $\text{KNO}_3$  (Figure 2c). In the solution containing  $\text{KClO}_4$  and  $\text{KPF}_6$  (Figure 2d,e), however, the electrode kinetics were slowed significantly, as indicated by the increased peak separations and the reduced peak currents. These results imply that charge transfer through the 1-adamantanethiol SAM depends on the anions. Electrochemical signals have been shown to depend on the anions present in cases of underpotential deposition<sup>22</sup> and conducting polymers,<sup>23</sup> in which anions were adsorbed onto a bare gold surface or acted

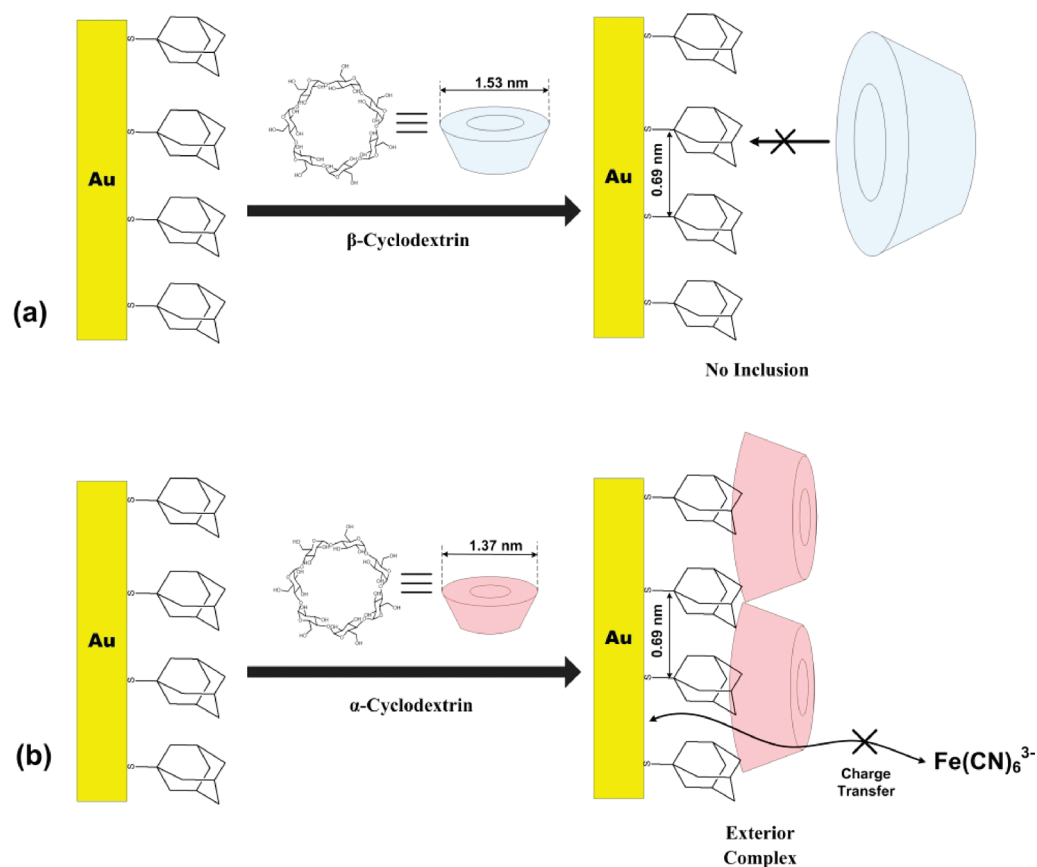
as counterions. The present system differed significantly because anions did not adsorb onto the 1-adamantanethiol SAMs, and reduction of ferricyanide did not require counteranions. No straightforward mechanism has been presented to explain this effect, but the anion-dependent properties of the SAM-modified gold resembled the sieving behavior of hydrated anions by nanoscopic pores.<sup>24</sup> Sieving behavior was observed when silver was deposited *via* underpotential deposition. Small hydrophilic anions with more affinity toward the bush of the decanethiol SAM (defects in the SAM acted as nanoscopic pores) enabled silver deposition, although large hydrophobic anions hindered silver deposition due to the anions' low affinity to pores in the SAM. Anions were not expected to pen-



Scheme 2. (a) Cell schematic of the electrolysis of ferricyanide; (b) balance sheet for the electrochemical cell with bare gold; and (c) diffusion portion of the balance sheet for the electrochemical cell with 1-adamantanethiol SAM-modified gold. The dashed arrows indicate the anion flux during electrolysis. The diffusive anion flux selectively passed through the nanoscopic sieve of the SAM. Anions are not drawn to scale.

strate the SAM pores during the ferricyanide redox reaction in our case. Careful consideration of the mass transfer of charged species by migration and diffusion, however, may provide insight into this anion effect. The electrolysis of ferricyanide on bare gold was considered, as shown in Scheme 2a. Assuming that the ionic conductivities ( $\lambda_i$ ) of all equivalent ions were equal, the transference numbers were as follows:  $t_{\text{K}^+} = 0.500$ ,  $t_{\text{ClO}_4^-} = 0.4985$ ,  $t_{\text{Fe(CN)}_6^{3-}} = 0.0015$ . The balance sheet<sup>20</sup> of the electrochemical cell on a bare gold surface is illustrated in Scheme 2b to demonstrate the flux of ionic species *via* migration and diffusion. Due to its high concentration, the supporting electrolyte carried most of the current in the bulk solution by migration, and most ferricyanide was transported to the cathode by diffusion. One of the most prominent fluxes was the diffusion of anions to the cathode, indicated by the dashed arrow in Scheme 2b. During electrolysis of ferricyanide on bare

gold, the supporting electrolyte anion diffused to the surface near the cathode to compensate the charge. In the absence of a SAM, the anions could move freely, as depicted in Scheme 2b. SAMs of 1-adamantanethiols, however, perturbed the flux of anions, as shown in Scheme 2c. Nanopores formed by defects in the SAM or the interstitial space between 1-adamantanethiols may have acted as nanoscopic sieves that selectively passed anions depending on the size and hydrophilic properties. Perturbation of the anion diffusion flux would have modified the double layer structure of the electrode or changed other mass transport characteristics of the balance sheet because the fluxes were mutually dependent. Therefore, the electrochemical signal would have been altered by the perturbed mass transport or modified double layer. In the present systems, the size of the anions increased and the hydration of the anions decreased in the following order:  $\text{Cl}^-$ ,  $\text{SO}_4^{2-}$ ,



**Scheme 3.** Illustrations of (a) the SAM of 1-adamantanethiol on gold and hindered binding with  $\beta$ -cyclodextrin, and (b) the formation of an exterior complex of  $\alpha$ -cyclodextrin and immobilized 1-adamantanethiol on gold. The geometry of the exterior complex is not drawn to scale.

$\text{NO}_3^-$ ,  $\text{ClO}_4^-$ ,  $\text{PF}_6^-$ .<sup>25,26</sup> In a solution containing the small anions chloride, sulfate, and nitrate, the redox reaction of ferricyanide showed electrochemically reversible kinetics, probably due to easy access of small anions to nanopores in the SAM. On the other hand, in a solution containing the large anions of perchlorate and hexafluorophosphate, the redox reaction of ferricyanide exhibited sluggish kinetics resulting from hindered mass transport due to the sieving behavior of the SAM toward these large anions. Though the size-selective mass transport of these non-electroactive ions does not change faradaic current directly, these results imply that the intrinsic properties of the anions, such as size and hydrophilicity, and the interaction with the 1-adamantanethiol SAM affect the electrochemical signal by perturbed diffusional flux of electroactive ions or modified double layer structure. Additionally, the SAM acted as a nanoscopic sieve with respect to anion diffusion flux.

**Electrochemical Study of the Adsorption of  $\alpha$ - and  $\beta$ -Cyclodextrins on a 1-Adamantanethiol SAM.** Adamantane is a guest molecule for  $\alpha$ - and  $\beta$ -cyclodextrin,<sup>27</sup> and surface-tethered adamantane is expected to display the same binding abilities toward the cyclodextrins. To measure the adsorption of  $\alpha$ - and  $\beta$ -cyclodextrin on the 1-adamantanethiol SAM, cyclic voltammetry was per-

formed in the presence of  $\alpha$ - and  $\beta$ -cyclodextrin. The binding of cyclodextrins to a monolayer of 1-adamantanethiol was expected to alter the environment of the electrode and observably affect the CV.<sup>28</sup> However, the voltammetric response was unchanged, even after immersion for several hours in a high concentration of 10 mM  $\beta$ -cyclodextrin, indicating that the  $\beta$ -cyclodextrin and the adamantane group on the surface did not interact. Faradaic impedance measurements were also unaffected in the absence and presence of  $\beta$ -cyclodextrin (Figures S1 and S2 in Supporting Information). The absence of host–guest complex formation may have resulted from the steric hindrance in the compact monolayer of 1-adamantanethiol. In previous scanning tunneling microscopy experiments,<sup>3,4</sup> the nearest neighbor distance of 1-adamantanethiol was found to be 0.69 nm. Because the outer diameter of  $\beta$ -cyclodextrin is 1.53 nm, close proximity of the adamantane groups may have prevented inclusion of  $\beta$ -cyclodextrin, as shown in Scheme 3a. In contrast, sluggish charge transfer was observed in cyclic voltammograms in the presence of  $\alpha$ -cyclodextrin. Figure 3 shows the CVs for the redox reaction of ferricyanide with several concentrations of  $\alpha$ -cyclodextrin. In the absence of  $\alpha$ -cyclodextrin, the CV in Figure 3a showed electrochemically quasi-reversible charge transfer.

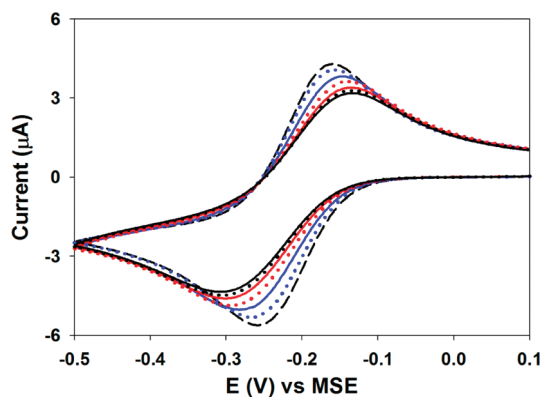


Figure 3. CVs for the redox reaction of 0.1 mM  $\text{Fe}(\text{CN})_6^{3-}$  containing 0.1 M  $\text{KClO}_4$  on 1-adamantanethiol SAM-modified gold in the presence of (a) 0 mM (black dashed line), (b) 3 mM (blue dotted line), (c) 10 mM (blue solid line), (d) 20 mM (red dotted line), (e) 30 mM (red solid line), (f) 40 mM (black dotted line), and (g) 50 mM (black solid line) of  $\alpha$ -cyclodextrin. The scan rate was 50 mV/s.

When the electrolyte contained a higher concentration of  $\alpha$ -cyclodextrin, a reduction in the faradaic current and an increased peak separation were observed, indicating that the adsorbed  $\alpha$ -cyclodextrin suppressed charge transfer to the ferricyanide molecules. These results demonstrated the formation of an exterior complex with adamantane where adamantane is positioned not at the cavity but at the outside of  $\alpha$ -cyclodextrin. In addition, the smaller diameter of  $\alpha$ -cyclodextrin, 1.37 nm, may have provided a denser adsorption layer on the 1-adamantanethiol SAM, diminishing charge transfer. Cucurbituril, a macrocyclic cage compound comprising six glycoluril units, can induce a similar effect on charge transfer when bound to a SAM composed of pseudorotaxane.<sup>29</sup> The dependence of the faradaic current on the concentration of  $\alpha$ -cyclodextrin in the electrolyte solution indicated that the  $\alpha$ -cyclodextrin coverage was closely related to the degree of blocking.

Quantitative measurements of this blocking behavior provided the adsorption isotherm of  $\alpha$ -cyclodextrin on a 1-adamantanethiol SAM.

Faradaic impedance experiments were performed to quantitatively measure the degree of blocking by the adsorbed  $\alpha$ -cyclodextrin.<sup>30–32</sup> As the concentration of  $\alpha$ -cyclodextrin increased, more  $\alpha$ -cyclodextrin was immobilized on the surface. The  $\alpha$ -cyclodextrin adsorbed onto the 1-adamantanethiol SAM suppressed charge transfer at the electrode, which increased the charge transfer resistance. Figure 4 shows that the impedance measurements on the 1-adamantanethiol SAM depended on the concentration of  $\alpha$ -cyclodextrin. The dramatic changes in the charge transfer resistance increment in the spectra demonstrated that the adsorption of  $\alpha$ -cyclodextrin obstructed charge transfer, and adsorption saturated near 50 mM  $\alpha$ -cyclodextrin. These spectra were modeled as Randles equivalent circuits consisting of a solution resistance ( $R_s$ ), charge transfer resistance ( $R_{ct}$ ), CPE, and Warburg impedance ( $Z_w$ ).<sup>33</sup> The diameter of the semicircle represented the  $R_{ct}$  at the electrode surface. The coverage of adsorbed  $\alpha$ -cyclodextrin was analyzed by assuming that the degree of blocking (*i.e.*, the charge transfer resistance) was proportional to the surface coverage of the adsorbed  $\alpha$ -cyclodextrin. The surface coverage was then estimated using the following simple relationship:

$$\Delta R_{ct} = R_{ct, [\alpha\text{-CD}]} - R_{ct, 0} = a\theta \quad (1)$$

where  $R_{ct, [\alpha\text{-CD}]}$  is the charge transfer resistance in a solution with a specific mole concentration of  $\alpha$ -cyclodextrin,  $R_{ct, 0}$  is the charge transfer resistance in a solution without  $\alpha$ -cyclodextrin,  $\theta$  is the adsorbed  $\alpha$ -cyclodextrin coverage, and  $a$  is the proportionality constant. Figure 5 shows the charge transfer resistance as a function of concentration of  $\alpha$ -cyclodextrin. The  $\alpha$ -cyclodextrin coverage increased gradually below 50

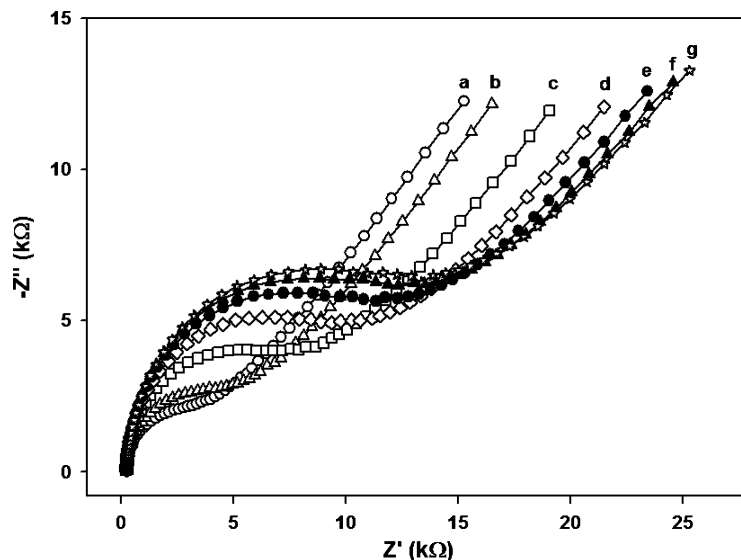


Figure 4. Impedance complex plots of the 1-adamantanethiol SAM on gold in the presence of 0.1 mM  $\text{Fe}(\text{CN})_6^{3-}$  and 0.1 M  $\text{KClO}_4$ , with (a) 0 mM, (b) 3 mM, (c) 10 mM, (d) 20 mM, (e) 30 mM, (f) 40 mM, and (g) 50 mM  $\alpha$ -cyclodextrin.

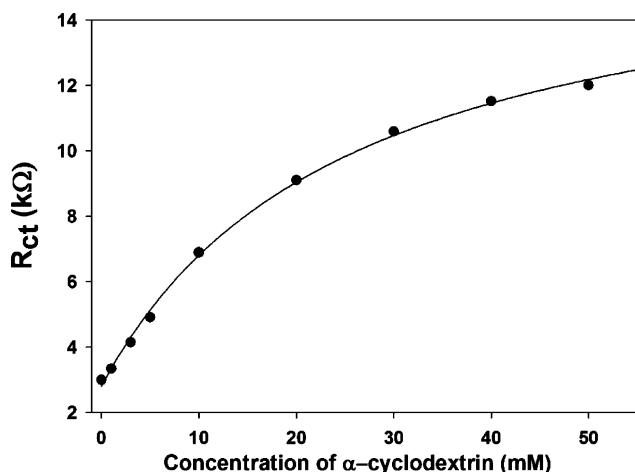


Figure 5. Charge transfer resistance vs concentration of  $\alpha$ -cyclodextrin. The continuous line shows the fit to eq 3.

mM. Above 50 mM,  $\alpha$ -cyclodextrin was fully bound to the available adamantane functional group. To understand the binding process, the adsorption data in Figure 5 were fit with a Langmuir isotherm model. The Langmuir isotherm as a function of surface coverage is

$$\theta = \frac{KC_{\alpha\text{-CD}}}{1 + KC_{\alpha\text{-CD}}} \quad (2)$$

where  $\theta$  is the coverage of the adsorbed  $\alpha$ -cyclodextrin,  $K$  is the apparent association constant for the formation of an exterior complex between adamantane and  $\alpha$ -cyclodextrin, and  $C_{\alpha\text{-CD}}$  is the molar concentration of  $\alpha$ -cyclodextrin in solution. Substituting eq 2 into eq 1 yields the following relationships

$$R_{\text{ct},[\alpha\text{-CD}]} - R_{\text{ct},0} = a\theta = \frac{aKC_{\alpha\text{-CD}}}{1 + KC_{\alpha\text{-CD}}}$$

$$R_{\text{ct},[\alpha\text{-CD}]} = R_{\text{ct},0} + \frac{aKC_{\alpha\text{-CD}}}{1 + KC_{\alpha\text{-CD}}} \quad (3)$$

The charge transfer resistance at a given  $\alpha$ -cyclodextrin concentration, which was determined

by the surface coverage of  $\alpha$ -cyclodextrin, was calculated from the measured charge transfer resistance via eq 3. As depicted in Figure 5, the resulting isotherms agreed with the experimental data. The binding constant obtained was  $39.53 \text{ M}^{-1}$ , which is three times smaller than the previously reported solution-based association constant of  $1.3 \times 10^2 \text{ M}^{-1}$ .<sup>12</sup> This result is in good agreement with previous reports that the association constant in host–guest chemistry decreases on the surface.<sup>14</sup>

## CONCLUSION

We studied the electrochemical properties of a 1-adamantanethiol SAM on a gold surface. Charge transfer through the 1-adamantanethiol SAM depended on the type of the anions. When ferricyanide was used as the redox probe and relatively large hydrophobic perchlorate and hexafluorophosphate anions were used as the supporting electrolytes, sluggish rates of charge transfer were observed. The charge transfer kinetics were nearly identical to those measured on a bare gold surface in the presence of chloride, sulfate, and nitrate supporting electrolytes. The driving force for this phenomenological result stemmed from the sieving effect of the 1-adamantanethiol SAM with respect to the diffusion flux of anions. The 1-adamantanethiol SAM could not bind  $\beta$ -cyclodextrin by the host–guest interaction, probably due to the small separation between neighboring adamantane molecules.  $\alpha$ -Cyclodextrin, in contrast, was immobilized by the formation of an exterior complex, as indicated by the suppressed charge transfer. This unique blocking property of the immobilized  $\alpha$ -cyclodextrin enabled us to quantify the amount of adsorbed  $\alpha$ -cyclodextrin using faradaic impedance experiments. The obtained adsorption isotherm was in good agreement with the Langmuir isotherm, and the binding constant was found to be  $39.53 \text{ M}^{-1}$ .

## EXPERIMENTAL METHODS

**Chemicals.**  $\alpha$ -Cyclodextrin was purchased from Fluka.

1-Adamantanethiol and all other chemicals (obtained from Aldrich or Sigma) were of analytical or better grade and were used as received. Ultrapure water ( $>18 \text{ M}\Omega$ ) from a Milli-Q water system (Millipore Corporation, Bedford, MA) was used throughout this work. All glassware and electrochemical cells were cleaned with Nochromix (Godax Lab., Inc.) cleaning solution and rinsed with ultrapure water.

**Incubation with Cyclodextrin.** Cyclodextrin solution was freshly prepared every day before an experiment. Cyclodextrin solution was injected in the electrochemical cell to make a cyclodextrin–adamantanethiol complex. After the 5 min incubation in room temperature, electrochemical measurements were performed. Five minutes is enough time to establish the equilibrium of adsorption which was checked by CVs (Figure S3 in Supporting Information). After the measurement, 1-adamantanethiol-modified gold electrode was washed with distilled water several times.

**Preparation of Self-Assembled Monolayers.** The gold substrates were prepared by thermal evaporation of a 5 nm thick titanium layer and a 100 nm gold layer onto a silicon wafer. Prior to use, the gold substrates were cleaned for 3 min in piranha solution (3:7 by volume 30%  $\text{H}_2\text{O}_2/\text{H}_2\text{SO}_4$ , *Caution: piranha solution reacts violently with most organic materials and must be handled with extreme care*), rinsed with  $\text{H}_2\text{O}$  and ethanol, and dried under a stream of argon. SAMs of 1-adamantanethiol were prepared by immersing the gold substrates in a 10 mM 1-adamantanethiol ethanol solution for at least for 24 h. After formation of the SAM, the substrates were rinsed several times with ethanol and dried under a stream of argon.

**Electrochemical Measurements.** Electrochemical experiments were performed using an Autolab potentiostat 10 (Ecochemie, The Netherlands). The three-electrode electrochemical cell consisted of the modified Au electrode, a Pt wire counter electrode, and a  $\text{Hg}/\text{Hg}_2\text{SO}_4$  (mercury sulfate electrode: MSE, saturated  $\text{K}_2\text{SO}_4$ ) reference electrode. The geometric area of the working electrode determined by the O-ring with 6 mm inner diameter



was estimated to be 0.283 cm<sup>2</sup>. The electrochemical impedance of the SAM-modified gold electrode was measured at 70 discrete frequencies per decade from 100 mHz to 2 kHz at an amplitude of 50 mV (rms) using an AUTOLAB FRA frequency response analyzer of the AUTOLAB 10. Impedance measurements were performed at a constant applied potential with respect to the formal potential of the redox probe. The semicircular diameters in the complex impedance plots ( $Z''$  vs  $Z'Z''$  = imaginary impedance and  $Z'$  = real impedance) corresponded to the interfacial charge transfer resistance ( $R_{ct}$ ), the values of which were calculated by a nonlinear least-squares (NLLS) fit using the program FRA. The impedance spectra were fit to a modified Randles equivalent electrical circuit, including the solution resistance ( $R_s$ ), a constant phase element (CPE), the charge transfer resistance ( $R_{ct}$ ), and the Warburg impedance ( $Z_w$ ).<sup>33</sup>  $R_s$  is the resistance of the electrolyte through which the current must pass. In parallel with  $R_{ct}$  is the non-faradaic electrode capacitance represented by a constant phase element (CPE) to take into account the microscopic roughness and atomic-scale inhomogeneities in the surfaces.  $R_{ct}$  was related to the kinetics of charge transfer at the SAM-modified gold surface.  $Z_w$  represents a type of resistance to mass transfer. Fitting constraints were imposed such that further iterations ceased when the variations in  $\chi^2$  were less than 0.001% compared with the previous iteration. The goodness of fit was assessed from the minimum  $\chi^2$ , the correlation matrix, and the relative error distribution plots. Deviations of less than 5% between the experimental and fitted data were assumed to be satisfactory for confirming the validity of the selected fitting circuit.

**Acknowledgment.** J.K. acknowledges the support from the Nano/Bio Science & Technology Program (2010-0008213) of the Ministry of Education, Science and Technology, and Basic Science Research Program through the National Research Foundation of Korea (NRF) funded by the Ministry of Education, Science and Technology (2010-0001951). S.H. acknowledges the support from Basic Science Research Program through the National Research Foundation of Korea (NRF) funded by the Ministry of Education, Science and Technology (2010-0015442) and the 2008 Research Fund of Myongji University.

**Supporting Information Available:** CVs and faradaic impedance measurements in the presence of  $\beta$ -cyclodextrin with 1-adamantanethiol SAM and CVs on 1-adamantanethiol SAM with various incubation times in the solution containing  $\alpha$ -cyclodextrin (as noted in the text). This material is available free of charge via the Internet at <http://pubs.acs.org>.

## REFERENCES AND NOTES

- Schleyer, P. v. R.; Williams, J. E.; Blanchard, K. R. The Evaluation of Strain in Hydrocarbons. The Strain in Adamantane and Its Origin. *J. Am. Chem. Soc.* **1970**, *92*, 2377–2386.
- Love, J. C.; Estroff, L. A.; Kriebel, J. K.; Nuzzo, R. G.; Whitesides, G. M. Self-Assembled Monolayers of Thiolates on Metals as a Form of Nanotechnology. *Chem. Rev.* **2005**, *105*, 1103–1169.
- Fujii, S.; Akiba, U.; Fujihira, M. Geometry for Self-Assembling of Spherical Hydrocarbon Cages with Methane Thiolates on Au(111). *J. Am. Chem. Soc.* **2002**, *124*, 13629–13635.
- Dameron, A. A.; Charles, L. F.; Weiss, P. S. Structures and Displacement of 1-Adamantanethiol Self-Assembled Monolayers on Au{111}. *J. Am. Chem. Soc.* **2005**, *127*, 8697–8704.
- Mullen, T. J.; Dameron, A. A.; Saavedra, H. M.; Williams, M. E.; Weiss, P. S. Dynamics of Solution Displacement in 1-Adamantanethiolate Self-Assembled Monolayers. *J. Phys. Chem. C* **2007**, *111*, 6740–6746.
- Dameron, A. A.; Mullen, T. J.; Hengstebeck, R. W.; Saavedra, H. M.; Weiss, P. S. Origins of Displacement in 1-Adamantanethiolate Self-Assembled Monolayers. *J. Phys. Chem. C* **2007**, *111*, 6747–6752.
- Saavedra, H. M.; Barbu, C. M.; Dameron, A. A.; Mullen, T. J.; Crespi, V. H.; Weiss, P. S. 1-Adamantanethiolate Monolayer Displacement Kinetics Follow a Universal Form. *J. Am. Chem. Soc.* **2007**, *129*, 10741–10746.
- Dameron, A. A.; Hampton, J. R.; Smith, R. K.; Mullen, T. J.; Gillmor, S. D.; Weiss, P. S. Microdisplacement Printing. *Nano Lett.* **2005**, *5*, 1834–1837.
- Gates, B. D.; Xu, Q.; Stewart, M.; Ryan, D.; Willson, C. G.; Whitesides, G. M. New Approaches to Nanofabrication: Molding, Printing, and Other Techniques. *Chem. Rev.* **2005**, *105*, 1171–1196.
- Braunschweig, A. B.; Huo, F.; Mirkin, C. A. Molecular Printing. *Nat. Chem.* **2009**, *1*, 353–358.
- Szejtli, J. Introduction and General Overview of Cyclodextrin Chemistry. *Chem. Rev.* **1998**, *98*, 1743–1753.
- Cromwell, W. C.; Byström, K.; Eftink, M. R. Cyclodextrin—Adamantanecarboxylate Inclusion Complexes: Studies of the Variation in Cavity Size. *J. Phys. Chem.* **1985**, *89*, 326–332.
- Ivanov, P. M.; Salvatierra, D.; Jaime, C. Experimental (NMR) and Computational (MD) Studies on the Inclusion Complexes of 1-Bromoadamantane with  $\alpha$ -,  $\beta$ -, and  $\gamma$ -Cyclodextrin. *J. Org. Chem.* **1996**, *61*, 7012–7017.
- Fukuda, T.; Maeda, Y.; Kitano, H. Stereoselective Inclusion of DOPA Derivatives by a Self-Assembled Monolayer of Thiolated Cyclodextrin on a Gold Electrode. *Langmuir* **1999**, *15*, 1887–1890.
- Michalke, A.; Janshoff, A.; Steinem, C.; Henke, C.; Sieber, M.; Galla, H.-J. Quantification of the Interaction between Charged Guest Molecules and Chemisorbed Monothiolated  $\beta$ -Cyclodextrins. *Anal. Chem.* **1999**, *71*, 2528–2533.
- Choi, S.-J.; Choi, B.-G.; Park, S.-M. Electrochemical Sensor for Electrochemically Inactive  $\beta$ -D-(+)-Glucose Using  $\alpha$ -Cyclodextrin Template Molecules. *Anal. Chem.* **2002**, *74*, 1998–2002.
- Fragoso, A.; Caballero, J.; Almirall, E.; Villalonga, R.; Cao, R. Immobilization of Adamantane-Modified Cytochrome c at Electrode Surfaces through Supramolecular Interactions. *Langmuir* **2002**, *18*, 5051–5054.
- Zeng, Q.; Marthi, R.; McNally, A.; Dickinson, C.; Keyes, T. E.; Forster, R. J. Host–Guest Directed Assembly of Gold Nanoparticle Arrays. *Langmuir* **2010**, *26*, 1325–1333.
- Crespo-Biel, O.; Dordi, B.; Reinhoudt, D. N.; Huskens, J. Supramolecular Layer-by-Layer Assembly: Alternating Adsorptions of Guest- and Host-Functionalized Molecules and Particles Using Multivalent Supramolecular Interactions. *J. Am. Chem. Soc.* **2005**, *127*, 7594–7600.
- Bard, A. J.; Faulkner, L. R. *Electrochemical Methods*, 2nd ed.; Wiley: New York, 2001; pp 137–155.
- Mullen, T. J.; Zhang, P.; Srinivasan, C.; Horn, M. W.; Weiss, P. S. Combining Electrochemical Desorption and Metal Deposition on Patterned Self-Assembled Monolayers. *J. Electroanal. Chem.* **2008**, *621*, 229–237.
- Herrero, E.; Buller, L. J.; Abruña, H. D. Underpotential Deposition at Single Crystal Surfaces of Au, Pt, Ag and Other Materials. *Chem. Rev.* **2001**, *101*, 1897–1930.
- Yang, H.; Kwak, J. Mass Transport Investigated with the Electrochemical and Electrogravimetric Impedance Techniques. 2. Anion and Water Transport in PMPy and PPy Films. *J. Phys. Chem. B* **1997**, *101*, 4656–4661.
- Lee, J.; Kwak, J. Sieving Behaviour of Nanoscopic Pores by Hydrated Ions. *Chem. Commun.* **2006**, 2167–2169.
- Conway, B. E. The Evaluation and Use of Properties of Individual Ions in Solution. *J. Solution Chem.* **1978**, *7*, 721–770.
- Robinson, R. A.; Stokes, J. M.; Stokes, R. H. Potassium Hexafluorophosphate—An Associated Electrolyte. *J. Phys. Chem.* **1961**, *65*, 542–546.
- Rekharsky, M. V.; Inoue, Y. Complexation Thermodynamics of Cyclodextrins. *Chem. Rev.* **1998**, *98*, 1875–1917.
- Kaifer, A. E. Interplay between Molecular Recognition and Redox Chemistry. *Acc. Chem. Res.* **1999**, *32*, 62–71.
- Kim, K.; Jeon, W. S.; Kang, J.-K.; Lee, J. W.; Jon, S. Y.; Kim, T.; Kim, K. A Pseudorotaxane on Gold: Formation of Self-Assembled Monolayers, Reversible Dethreading and

- Rethreading of the Ring, and Ion-Gating Behavior. *Angew. Chem., Int. Ed.* **2003**, *42*, 2293–2296.
30. Kim, K.; Kwak, J. Faradaic Impedance Titration of Pure 3-Mercaptopropionic Acid and Ethanethiol Mixed Monolayers on Gold. *J. Electroanal. Chem.* **2001**, *512*, 83–91.
  31. Hwang, S.; Lee, B. S.; Chi, Y. S.; Kwak, J.; Choi, I. S.; Lee, S.-g. Faradaic Impedance Titration and Control of Electron Transfer of 1-(12-Mercaptododecyl)imidazole Monolayer on a Gold Electrode. *Electrochim. Acta* **2008**, *53*, 2630–2636.
  32. Lee, J. A.; Hwang, S.; Kwak, J.; Park, S. I.; Lee, S. S.; Lee, K.-C. An Electrochemical Impedance Biosensor with Aptamer-Modified Pyrolyzed Carbon Electrode for Label-Free Protein Detection. *Sens. Actuators, B* **2008**, *129*, 372–379.
  33. Randles, J. E. B. Kinetics of Rapid Electrode Reactions. *Discuss. Faraday Soc.* **1947**, *1*, 11–19.